Optics Communications 495 (2021) 127085

Contents lists available at ScienceDirect

Optics Communications

journal homepage: www.elsevier.com/locate/optcom

Passively Q-switched semiconductor disk laser with microsecond pulse duration

Peng Zhang [a,*], Xiaojian Zhang [a], Renjiang Zhu [a], Lijie Wang [b], Tao Wang [a,*]

[a] College of Physics and Electronic Engineering, Chongqing Normal University, Chongqing 401331, People's Republic of China
[b] State Key Laboratory of Luminescence and Applications, Changchun Institute of Optics, Fine Mechanics and Physics, Chinese Academy of Sciences, Changchun, Jilin 130033, People's Republic of China

ARTICLE INFO

Keywords:
Passively Q-switched
Semiconductor disk laser
Saturable absorber
Cr^{4+}:YAG crystal
Semiconductor saturable absorb mirror

ABSTRACT

A semiconductor disk laser was passively Q-switched by the use of a Cr^{4+}:YAG crystal and a semiconductor saturable absorb mirror, respectively, and stable Q-switched laser pulse trains with microsecond pulse duration were produced. The width and the repetition rate of the Q-switched pulses were 10 μs and 26.3 kHz when a Cr^{4+}:YAG crystal was inserted, while the pulse width and the repetition rate were 8 μs and 26.3 kHz when a semiconductor saturable absorb mirror was employed. Based on the time characteristics of the quantum structure in the active region of the semiconductor disk laser, and the time behaviors of the saturable absorbers, i.e., the Cr^{4+}:YAG crystal and the semiconductor saturable absorb mirror, the formatting mechanisms of the Q-switched pulses with width of microsecond magnitude were analyzed, and the related physical pictures of the passively Q-switched semiconductor disk laser were further disclosed.

1. Introduction

Q-switch technology are widely used in solid state lasers to produce giant pulses with nanosecond duration, kilohertz repetition rate and megawatt peak power, which are highly required in scientific researches [1], laser medicines [2], industrial processes [3] and so on. For semiconductor lasers, on the one hand, the life time of carriers is of nanosecond magnitude, considerably lower than the life time (varies from microseconds to milliseconds) of the iron doped in gain medium of a solid state laser, so the giant pulses could not be obtained directly. But on the other hand, the nanosecond life time of carriers in a semiconductor laser supports a repetition rate of the Q-switched pulses as high as gigahertz, and these pulse train can find important applications in fields such as high-speed communications and high-speed electro-optic sampling.

Different from the active Q-switch including the electro-optic Q-switch and acousto-optic Q-switch, and the passive Q-switch used in a solid state laser, Q-switched semiconductor lasers employ two-section configuration, i.e., there are two sections separated by a waveguide region in a laser, one section is the general active region, and the other works as an absorber, or named modulator. These Q-switched semiconductor lasers can produce stable laser pulse train with sub-nanosecond width and gigahertz repetition rate [4–7]. As to shorter pulses with picosecond or femtosecond duration, another two technologies, gain-switch [8] and mode-lock [9], have to be introduced in a semiconductor laser. The shortcoming of relatively low output power of a Q-switched semiconductor laser can be compensated partly if a master oscillator power amplifier is applied. Given its advantages such as compactness, reliability, tunability and tailorable wavelength, applications of Q-switched semiconductor lasers could be further extended.

Semiconductor disk lasers (SDLs), also called optically pumped vertical external cavity surface emitting lasers (VECSELs), comprise the similar gain structure of a vertical cavity surface emitting laser (VCSELs) and the same geometry configuration of a solid state disk lasers, and can produce high output power and good beam quality simultaneously [10–13]. It has been successfully used in nonlinear frequency conversion [14,15], ultra-short pulse generation [16,17], terahertz time domain spectrometer [18], life sciences [19], laser medicine [20], etc.

To the best of our knowledge, Q-switch in a SDL has not been investigated either experimentally or theoretically so far. In this paper, a SDL is passively Q-switched by a Cr^{4+}:YAG crystal and a semiconductor saturable absorb mirror (SESAM), respectively. The experimental results are analyzed based on the time characteristics of the quantum wells in the active region of the SDL, as well as the time behaviors of the saturable absorbers (i.e., the Cr^{4+}:YAG crystal and the SESAM), and the formatting mechanisms of the Q-switched pulses with microsecond duration are proposed.

* Corresponding authors.
E-mail addresses: zhangpeng2010@cqnu.edu.cn (P. Zhang), wangt@cqnu.edu.cn (T. Wang).

https://doi.org/10.1016/j.optcom.2021.127085
Received 1 February 2021; Received in revised form 29 April 2021; Accepted 30 April 2021
Available online 5 May 2021

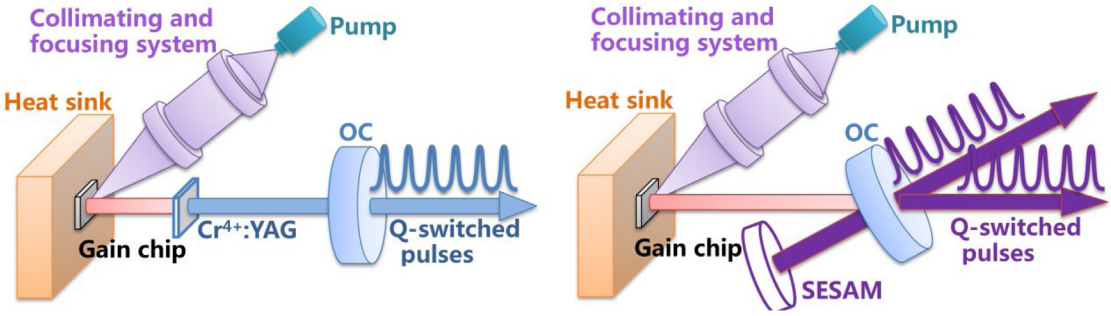

Fig. 1. Schematics of the passively Q-switched SDL with a Cr^{4+}:YAG crystal (left) and a SESAM (right).

2. Experimental setup

The gain chip used in the SDL is epitaxially grown in reverse sequences. Firstly, an etch stop layer of AlGaAs with high Al composition is deposited on GaAs substrate, then a GaAs protect layer is grown. Subsequently, an AlGaAs layer with high barrier to prevent the carriers from surface recombination is introduced, and the next is an active region consisting of multiple quantum wells. There are twelve InGaAs/GaAsP quantum wells in the active region, and the content of In in InGaAs is designed to meet the target laser wavelength of 980 nm. Since the GaAsP layer would play three roles (i.e., the strain compensation layer, the barrier layer, and the pump absorbing layer) in the active region, so the content of P in GaAsP must be adequate to compensate the strain, and meanwhile, cannot be too much to absorb the pumping energy.

Above the active region is the distributed Bragg reflector (DBR), which is composed of 30 pairs alternate AlGaAs layers with high Al (lower refractive index) and low Al (higher refractive index) composition. The designed center wavelength and high-reflectivity bandwidth of the DBR are 980 nm and 100 nm respectively. The entire epitaxial wafer is ended by an antioxidant GaAs layer. In a SDL, the DBR at the bottom and the semiconductor–air interface at the front of the chip form a microcavity, and this will result in a laser standing wave in the active region. In order to get higher gain coefficient, the thickness of every single layer in the wafer, especially layers of multiple quantum wells, should be designed and grown accurately to ensure that all quantum wells are located at the antinodes of the standing wave, so to form a resonant periodic gain structure [21].

The grown wafer is split to small chips with 4 mm × 4 mm dimension. The epitaxial end face of the chip is metalized with titanium–platinum–aurum sequentially, then the chip is bonded to a copper heatsink, and the substrate is removed using chemical etch.

As a frequently used passive Q-switch crystal, the Cr^{4+}:YAG crystal used in our experiment has a thickness of 1.6 mm and an absorption coefficient of 4.5% at 980 nm laser wavelength. Both transparent surfaces of the crystal are antireflection coated, and the reflectivity of the surface is small than 0.185% at 980 nm wavelength.

The primary technical parameters of the SESAM employed in this work are as following: the absorption wavelength of the quantum well is 980 nm, the range of high-reflectivity (R > 96%) of the BDR lies between 910 and 990 nm, the modulation depth $\Delta R = 1.2\%$, the saturated absorption coefficient $A_0 = 2.0\%$, the non-saturated loss $A_{ns} = 0.8\%$, the saturated flux $\Phi_{sat} = 120\ \mu J/cm^2$, and the relaxation time τ_s~500 fs.

On the left of Fig. 1, a straight linear cavity passively Q-switched SDL with Cr^{4+}:YAG crystal is depicted. Pumping light from a fiber-coupled 808 nm semiconductor laser is collimated and then focused on the gain chip at an incident angle of about 30 degrees. A flat-concave mirror with 100 mm curvature radius is applied as the external output coupler (OC). The OC is high-reflection coated and has a reflectivity of about 99.9% at 980 nm wavelength. To get higher power density of incident light on the crystal, so to build better absorption and achieve saturation earlier, the Q-switch crystal is placed to the gain chip as near as possible during the experiment.

The folded cavity passively Q-switched SDL using a SESAM is shown on the right of Fig. 1. The folded mirror, that is to say the OC, has a curvature radius of 50 mm and is high-reflection coated at 980 nm laser wavelength. In order to produce tighter focus of light on the SESAM, so to meet the requirement of saturation of the SESAM and start the process of Q-switching, the cavity length of the arm containing the gain chip should be longer than that of the arm with the SESAM. In the experiment, the lengths of the gain arm and the SESAM arm are chosen in a way that the area ratio of the light spot on the gain chip to the light spot on the SESAM is about 20:1.

3. Results and discussions

3.1. Continuous wave SDL

As shown on the left of Fig. 1, if the Cr^{4+}:YAG crystal is not inserted, the laser will work in continuous wave (CW).

Fig. 2 shows the output powers of the CW SDL with different pump powers under room temperature (25 °C). The slope efficiency (SE) of the laser is about 9.4%, and the maximum output power is 924 mW when the pump power reaches 11.9 W. After that, increasing pump power would lead to a dropping output power because of the thermal effects. The principal reason for the relatively low output power of the CW SDL is the small transmission (i.e., output couple coefficient) of about 0.1% of the OC. It is clear that lower transmission means higher intra-cavity circling power, which may accelerate the thermal effect in the active region, decrease the gain of the quantum wells, and cause the thermal rollover of the laser. If an OC with properly higher transmission is selected, higher SE and larger maximum output power of the SDL could be expected.

The photoluminescence of gain chip under 1.2 W pump power and the laser spectrum of SDL under 5.6 W pump power are plotted in the inset of Fig. 2. Considering that the emitting wavelength of InGaAs quantum wells will redshift with a rate of about 0.3 nm/K when the SDL works under intense pump and the temperature in the active region goes up, the designed emitting wavelength of InGaAs quantum wells under weak pump is 965 nm, so that when the quantum wells are heated to the desired value of 350 K by the rising pump, its emitting wavelength shift just to the expected laser wavelength of 980 nm. It can be seen from the inset of Fig. 2 that the emitting wavelength of quantum wells under weak pump is 963.5 nm, very close to the designed value of 965 nm.

When the pump power is increased to 5.6 W, the measured laser wavelength is 971 nm, and the full width at half maximum (FWHM) of the laser spectrum is about 1.1 nm. The obvious redshift of the wavelength indicates a significant temperature rise in the active region, which suggests a serious thermal effect in the gain chip, and this is partly caused by the use of a high reflectivity OC, just as mentioned before.

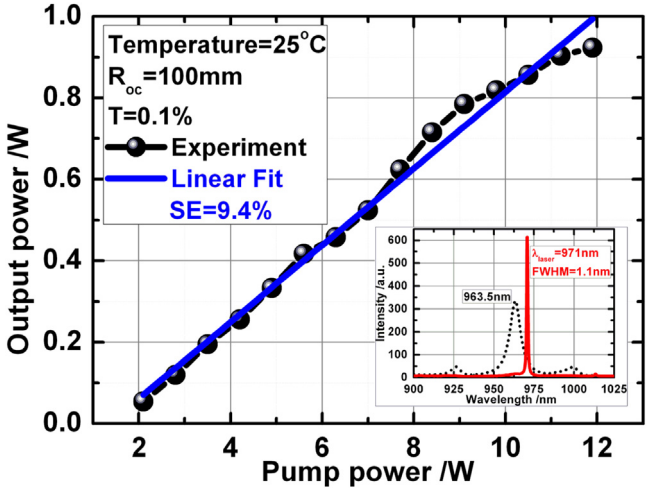

Fig. 2. Output powers vs. pump powers of the CW SDL under room temperature. The inset is the photoluminescence of gain chip under weaker pump and the laser spectrum of SDL under intenser pump.

To characterize the beam quality of the laser, M^2 factor of the output beam has been measured under condition of 25 °C temperature and 9.8 W pump power, and the results are shown in Fig. 3. The values of M^2 factor in the X and Y directions are 1.00 and 1.02, respectively, which shows a good beam quality of the laser.

3.2. Passively Q-switched SDL

In accordance with the left of Fig. 1, a laser cavity is set up and a Cr^{4+}:YAG crystal is placed to the gain chip as near as possible to obtain a smaller light spot on the crystal, so to get a higher power density of incident light and meet the requirement of the saturation in the absorber. The left of Fig. 4 shows a stable pulse train of the Cr^{4+}:YAG Q-switched SDL under room temperature and 4.5 W pump power. The pulse width is 10 μs and the pulse period is 38 μs, corresponding to a repetition rate of 26.3 kHz.

SESAM is widely used as the saturable absorber to realize mode-locked operation in a SDL or a solid-state laser, it is also often employed in a solid-state laser to achieve Q-switched running. But to our best knowledge, it is introduced in a SDL to implement Q-switching for the first time. The different requirement of the SESAM between achieving Q-switched and mode-locked operation in a SDL is: when a SESAM is utilized as a Q-switch, the saturable absorption is based on the inter-band relaxation of the carriers. It is necessary to satisfy the condition that SESAM saturation precedes gain saturation, i.e., the laser spot on SESAM should be smaller than that on gain chip. While a SESAM is employed as a mode-locked element, the saturable absorption relies on the intraband relaxation of the carriers. A steady mode-locking requires strict intracavity dispersion relation and tighter focus of laser spot on the SESAM.

By using a SESAM as the saturable absorber, the passively Q-switched SDL with configuration shown on the right side of Fig. 1 is performed, and the output steady pulse train is demonstrated on the right side of Fig. 4 when the temperature is 300 K and the pump power is 4.5 W. The pulse width is 8 μs and the pulse period is 38 μs, corresponding to a repetition rate of 26.3 kHz, same as that in the Cr^{4+}:YAG Q-switched SDL.

Although laser pulses with duration of microsecond magnitude from Q-switched solid state laser and fiber laser have been reported [22,23], pulses shown in Fig. 4 are quite different from those of a typical Q-switched solid state laser. For a typical Q-switched solid state laser, the pulse width varies from a few nanoseconds to a dozen nanoseconds, and the pulse period is between tens of microseconds and hundreds of microseconds. As to the passively Q-switched SDL, the pulse width and the pulse period are of same magnitude of microseconds. This difference primarily originates from the time characteristics of the gain medium in a solid state laser, as well as the multiple quantum wells in a SDL, along with the saturable absorber used for Q-switching, and the reasons of this difference will be discussed in more detail later.

In Fig. 4, the outline of Q-switched pulses on the right is not as smooth as it shown on the left, we think the possible reasons are: the relaxation time of Cr^{4+}: YAG crystal is about 3–4 μs, which is in the same order of magnitude of the pulse width. So, in the process of pulse formation, change of the crystal transmittance is smooth, and then followed the smoothly changed carriers in gain medium, further the smooth variation of photon number in resonant cavity, which means a smooth profile of the output pulse train. For the case of SESAM Q-switching, however, the relaxation time of SESAM τ~500 fs, is far less than the pulse width. Therefore, in the process of pulse formation, the reflectivity of SESAM still rises and falls frequently in the short term on the basis of long-term saturation. This results in the fluctuation of the transmittance of SESAM, the quickly change of the number of carriers in gain medium, and the corresponding change of the photon number in resonant cavity, which are consistent with a rougher pulse outline, just as can be seen from the right of Fig. 4.

Fig. 5 shows the relationship of output powers and different pump powers when a SDL is Q-switched by a SESAM under room temperature. With 7.2 W pump power, the maximum output power of 33 mW is obtained, and the pulse repetition rate is 58.1 kHz, indicating single-pulse energy of 0.57 μJ. The saturated absorption coefficient of the SESAM is 2.0%. In addition to that, there are two output laser beams in the folded cavity. For this reason, we think that the high cavity loss is the main cause of the relatively low output power from the SEAM Q-switched SDL, and the use of a SESAM with optimized less saturated absorption coefficient and smaller modulation depth would support higher SE and maximum output power.

Connections between pulse periods and pump powers of the Q-switched SDL under room temperature are show in Fig. 6. Two different kinds of fitting, reciprocal and exponential fitting, for experimental data are carried out, and the correlation coefficients R^2 of the reciprocal and exponential fitting are 0.96 and 0.99, respectively. We adopt the latter exponential fitting, which means that the pulse period in a Q-switched SDL decrease quickly and reach a saturation value earlier comparing to that in a Q-switched solid state laser (In a typical passively Q-switched solid state laser, the pulse repetition rate rises linearly with increasing pump power [24,25], i.e., the pulse period fall reciprocally with the increasing pump power.). This is a deducible result because in a solid state laser, the pulse duration and period are of nanosecond and microsecond magnitude and the duty circle is of 10^{-3} magnitude, lots of new pulses could grow out between two old pulses when the pump power goes up. However, in a SDL, the pulse duration and period are all of microsecond magnitude and the duty circle is of 10^{-1} magnitude, the capability of two adjacent pulses to accommodate more new pulses is very limited, and this is the reason for why the pulse repetition rate also increase with increasing pump power, but get saturation status earlier.

3.3. Mechanism of the Q-switched pulses with μs duration

In a typical passively Q-switched solid state laser, the relaxation time τ_s of the absorption crystal Cr^{4+}:YAG is approximately 3~4 μs [26,27], while the life time τ of the upper level of gain medium changes from hundreds of microsecond to millisecond, which is 2~3 orders of magnitude higher than the relaxation time of the absorber. So the population inversion density n can be accumulated easier, the ratios of initial population density to final population density n_i/n_f, and initial population density to threshold population inversion density n_i/n_t are all higher. When the build-up of the laser pulse starts, the absorber will be bleached very quickly and giant pulses with nanosecond duration could be produced. Previous dynamic simulations [28] have

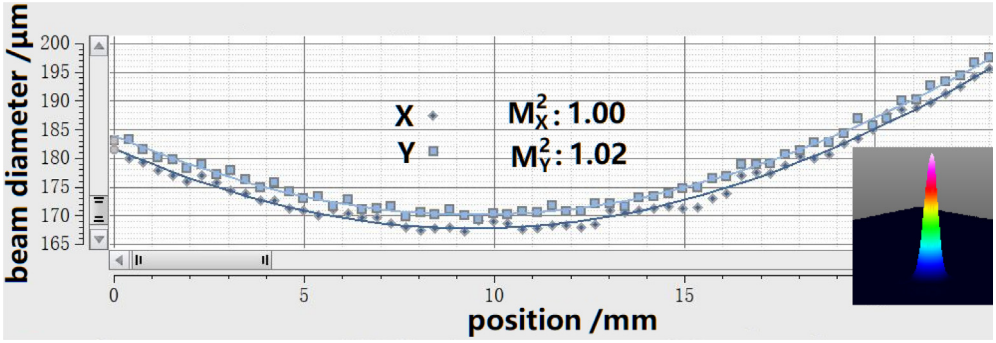

Fig. 3. M^2 factor of the output beam under condition of 25 °C temperature and 9.8 W pump power. The inset is the 3D distribution of the laser intensity.

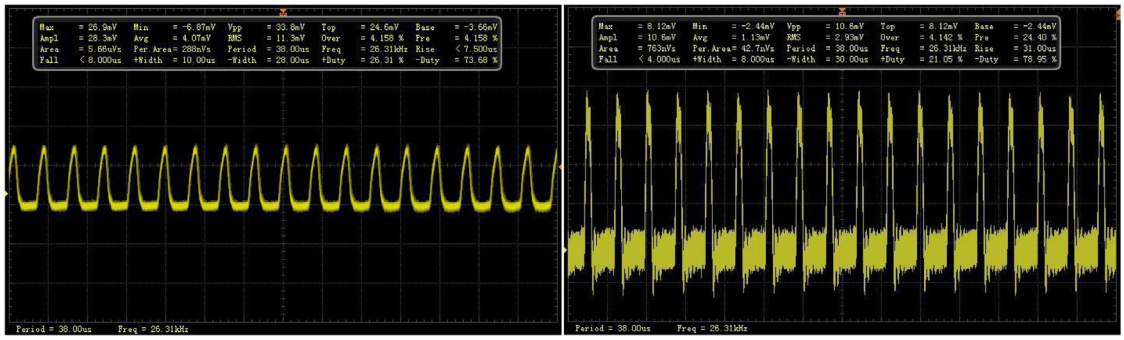

Fig. 4. Pulse train from the Cr^{4+}:YAG Q-switched SDL (left) and the SESAM Q-switched SDL (right) under room temperature.

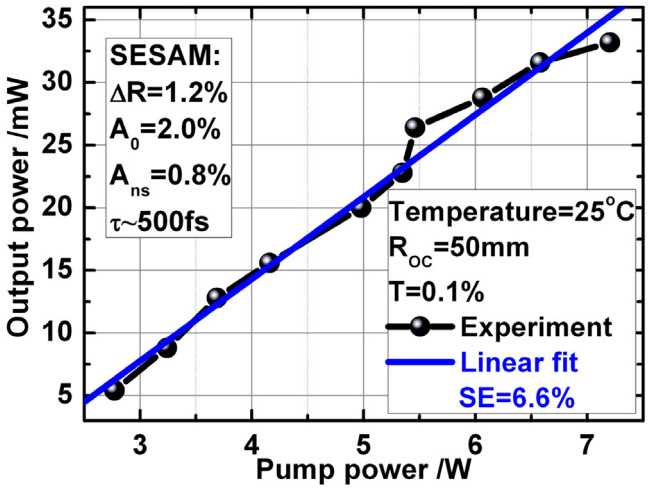

Fig. 5. Relationship of output powers and different pump powers when the SDL is Q-switched by a SESAM under room temperature.

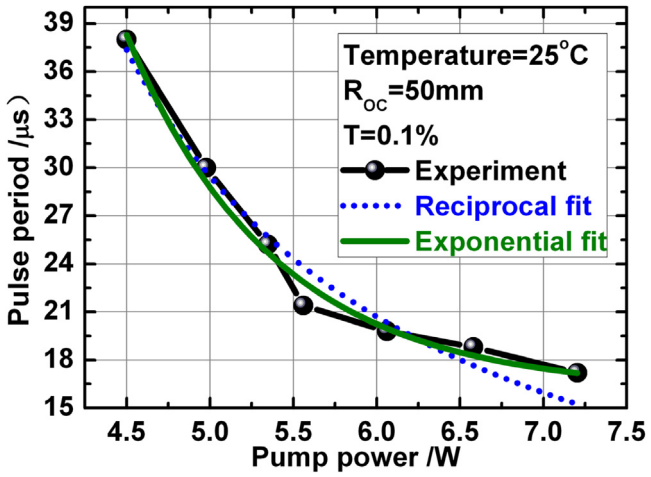

Fig. 6. Pulse periods of a SESAM Q-switched SDL with different pump powers under room temperature.

demonstrated that the period of the stable pulse train from a passively Q-switched solid state laser is about tens or hundreds of microsecond, and the repetition rate is of kilohertz magnitude.

But this case is not applicable to a passively Q-switched SDL. For a SDL, the life time of carriers is of nanosecond magnitude [29,30], the accumulation of carriers in conduction band is quite slow, and the values of n_i/n_f and n_i/n_t are all smaller. After the build-up of the laser pulse begins, the process of being bleached in the absorber is much slower, resulting in a pulse train with duration of microsecond magnitude, as can be seen in Fig. 4. Furthermore, it can be concluded that these microsecond pulses are principally cause by the time behavior of carriers in the gain chip of a SDL, whereas the influence of time properties of the saturable absorber on the Q-switched pulses is not obvious, and this can be proved by Fig. 4, too.

To further confirm the above statements, rate equations of general passively Q-switched lasers can be used here. The evolution of the photon density φ in laser cavity, the instantaneous population inversion density n in gain medium, and the instantaneous population density of the absorbing state n_s in absorber can be written as [31,32]

$$\frac{d\phi}{dt} = \left[2\sigma nl - 2\sigma_s n_s l_s - \left(\ln(\frac{1}{R}) + L\right)\right]\frac{\phi}{t_r} \quad (1)$$

$$\frac{dn}{dt} = -\gamma\sigma c\phi n \quad (2)$$

$$\frac{dn_s}{dt} = -\gamma_s\sigma_s c\phi n_s \quad (3)$$

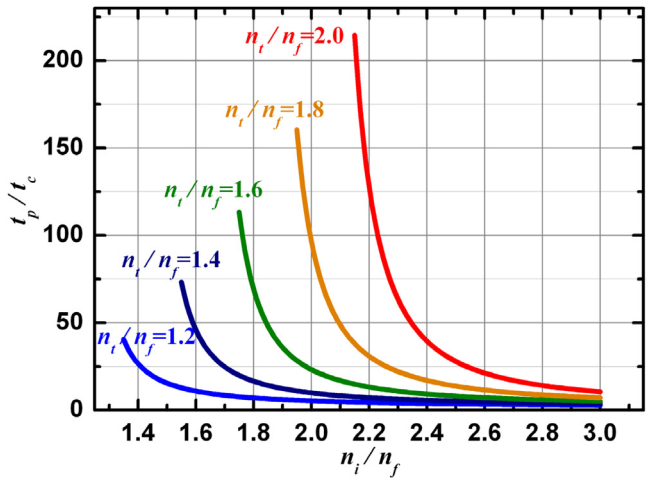

Fig. 7. Change of pulse duration t_p/t_c with n_i/n_f for different n_t/n_f.

where σ and σ_s are the stimulated emission section of laser and the absorption cross section of absorber, respectively. l and l_s are the lengths of gain medium and absorber. c is the speed of light, t_r is the round-trip transit time of light in cavity, R is the reflectivity of OC, and L is the remaining two way dissipative optical loss. γ and γ_s are the degeneracy factors of gain medium and absorber, respectively.

The pulse duration could be derived from the above rate equations and can be express as [33]

$$t_p = t_c \frac{n_i - n_f}{n_i - n_t\left[1 + \ln\left(\frac{n_i}{n_t}\right)\right]} \tag{4}$$

where the photon decay time t_c is

$$t_c = \frac{t_r}{\ln\left(\frac{1}{R}\right) + L} \tag{5}$$

It is clear that pulse width of a Q-switched laser would be affected by the values of n_i/n_f and n_i/n_t significantly. According to the experiment described before, using the parameters of $R = 99.9\%$, $L = 2.2\%$ (for SESAM Q-switch), and a cavity length of 100 mm, the calculated photon decay time t_c is about 30 ns. We plot the change of pulse duration t_p/t_c with n_i/n_f for different n_t/n_f in Fig. 7. It can be verified from Fig. 7 that lower value of n_i/n_f and higher value of n_t/n_f (which means lower n_i/n_t) may push the pulse duration from nanosecond magnitude to microsecond magnitude, and this is what happened we believe in a passively Q-switched SDL.

According to the different magnitude of the pulse duration, the Q-switching area can be divided into three parts: the nanosecond region, the transition region and the microsecond region if we refer a pulse with duration $t_p/t_c < 10$ (i.e., duration < 300 ns) as nanosecond pulse and a pulse with duration $t_p/t_c > 100$ (i.e., duration > 3 μs) as microsecond pulse, just as shown in Fig. 8. It can be said that the values of n_i/n_f and n_t/n_f of a passively Q-switched SDL are situated in the microsecond region.

4. Conclusions

We have presented a SDL passively Q-switched by a Cr^{4+}:YAG crystal and a SESAM respectively. The pulse widths of Cr^{4+}:YAG and SESAM Q-switched SDL are 10 μs and 8 μs with same repetition rate of 26.3 kHz when the pump power is 4.5 W and the temperature is 25 °C. The maximum output power of 33 mW is obtained from SESAM Q-switched SDL with 7.2 W pump power, and the pulse repetition rate is 58.1 kHz, corresponding to single-pulse energy of 0.57 μJ. With increasing pump power, the pulse period decrease exponentially in a Q-switched SDL instead of reciprocally in a typical Q-switched solid state laser. A formula of pulse width derived from the rate equations is used to explain the behavior of the pulse train from the Q-switched SDL, and it is found that the lower values of n_i/n_f and n_t/n_f in the gain medium, which is mainly risen from the time characteristics of quantum wells in active region, is the reason for why the pulse duration is of microsecond magnitude. Seeing that SDLs can produce high output power and good beam quality simultaneously, these compact, wavelength tailorable passively Q-switched SDLs could be applied in frequency conversion, fluorescence excitation, laser medicine and so on, after the average output power of laser is improved and the pulse peak power is upgraded.

Declaration of competing interest

The authors declare that they have no known competing financial interests or personal relationships that could have appeared to influence the work reported in this paper.

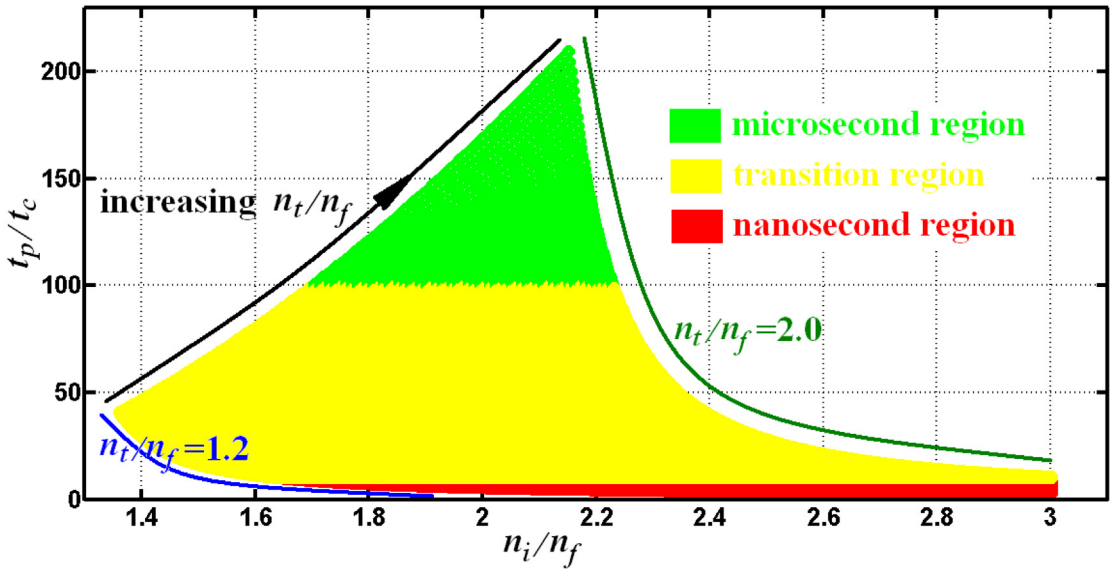

Fig. 8. Schematics of the three different regions according to different magnitude of pulse duration.

Acknowledgments

This work is supported by the Science and Technology Research Program of Chongqing Municipal Education Commission, China (KJZD-M201900502), the National Natural Science Foundation of China (61904024), the Chongqing Research Program of Basic Research and Frontier Technology, China (cstc2018jcyjAX0319), the "Blue Fire Plan" (Huizhou) Foundation of Industry-University-Research Joint Innovation of Ministry of Education, China (CXZJHZ201728), State Key Laboratory of Luminescence and Applications, China (SKLA-2019-04), and the Scientific and Technological Research Program of Chongqing Municipal Education Commission, China (KJQN201800528).

References

[1] E.C. Honea, R.J. Beach, S.C. Mitchell, P.V. Avizonis, 183-w, m^2=2.4 yb:yag q-switched laser, Opt. Lett. 24 (1999) 154–156.
[2] M.A. Latina, S.A. Sibayan, D.H. Shin, R.J. Noecker, G. Marcellino, Q-switched 532-nm nd:YAG laser trabeculoplasty (selective laser trabeculoplasty): a multicenter, pilot, clinical study, Ophthalmology 105 (1998) 2082–2090.
[3] J.J. Zayhowski, Passively Q-switched nd:YAG microchip lasers and applications, J. Alloy. Compd. 303 (2000) 393–400.
[4] Y.A. Drozhbin, Y.P. Zakharov, V.V. Nikitin, A.S. Semenov, V.A. Yakovlev, Generation of ultrashort light pulses with a gaas semiconductor laser, JETP Lett. 5 (1967) 143–145.
[5] T.P. Lee, R. Roldan, Repetitively Q-switched light pulses from gaas injection lasers with tandem double-section stripe geometry, IEEE J. Quantum Electron. 6 (1970) 339–352.
[6] D.Z. Tsang, J. Walpole, Q-switched semiconductor diode lasers, IEEE J. Quantum Electron. 19 (1983) 145–156.
[7] B. Cakmak, Modelling of experimentally measured Q-switched pulsations in ingaas/gaas diode lasers, Opt. Commun. 266 (2006) 614–619.
[8] K.Y. Lau, Gain switching of semiconductor injection lasers, Appl. Phys. Lett. 52 (1988) (1988) 257–259.
[9] P.P. Vasilev, I.H. White, J. Gowar, Fast phenomena in semiconductor lasers, Rep. Progr. Phys. 63 (2000) 1997–2042.
[10] M. Kuznetsov, F. Hakimi, R. Sprague, A. Mooradian, Design and characteristics of high-power (>0.5-w CW) diode-pumped vertical-external-cavity surface- emitting semiconductor lasers with circular tem_{00} beams, IEEE J. Sel. Top. Quantum 5 (1999) 561–573.
[11] A.C. Tropper, S. Hoogland, Extended cavity surface-emitting semiconductor lasers, Prog. Quant. Electron. 30 (2006) 1–43.
[12] A. Rahimi-Iman, Recent advances in VECSELs, J. Optics-UK 18 (2016) 093003.
[13] M. Guina, A. Rantamäki, A. Härkönen, Optically pumped VECSELs: review of technology and progress, J. Phys. D Appl. Phys. 50 (2017) 383001.
[14] S. Calvez, J.E. Hastie, M. Guina, O.G. Okhotnikov, M.D. Dawson, Semiconductor disk lasers for the generation of visible and ultraviolet radiation, Laser Photonics Rev. 3 (2009) 407–434.
[15] J.E. Hastie, L.G. Morton, A.J. Kemp, M.D. Dawson, A.B. Krysa, J.S. Roberts, Tunable ultraviolet output from an intracavity frequency-doubled red vertical-external-cavity surface-emitting laser, Appl. Phys. Lett. 89 (2006) 061114.
[16] U. Keller, A.C. Tropper, Passively mode-locked surface-emitting semiconductor lasers, Phys. Rep. 429 (2006) 67–120.
[17] C.G. Alfieri, D. Waldburger, J. Nürnberg, M. Golling, U. Keller, Sub-150-fs pulses from an optically pumped broadband mode-locked integrated external-cavity surface emitting laser, Opt. Lett. 44 (2019) 25–28.
[18] Z. Mihoubi, K.G. Wilcox, S. Elsmere, A. Quarterman, R. Rungsawang, I. Farrer, H.E. Beere, D.A. Ritchie, A. Tropper, V. Apostolopoulos, All-semiconductor room- temperature terahertz time domain spectrometer, Opt. Lett. 33 (2008) 2125–2127.
[19] E. Esposito, S. Keatings, K. Gardner, J. Harris, G. Mcconnell, Confocal laser scanning microscopy using a frequency doubled vertical external cavity surface emitting laser, Rev. Sci. Instrum. 79 (2008) 083702.
[20] E. Kantola, A. Rantamaki, I. Leino, J.P. Penttinen, M. Guina, VECSEL-Based 590-nm laser system with 8 w of output power for the treatment of vascular lesions, IEEE J. Sel. Top. Quantum 25 (2018) 1–8.
[21] S.W. Corzine, R.S. Geels, J.W. Scott, R.H. Yan, L.A. Coldren, Design of Fabry-Perot surface-emitting lasers with a periodic gain structure, IEEE J. Quantum Electron. 25 (1989) 1513–1524.
[22] T. Rui, G. Zi-ye, W. Zheng-mao, X. Guang-qiong, Output characteristics of diode-pumped passively Q-switched yb:$Cayalo_4$ pulsed laser based on a SESAM, Chinese Optics 12 (2019) 167–178.
[23] Z.T. Wang, Y.H. Zou, Y. Chen, M. Wu, S.C. Wen, Graphene sheet stacks for Q-switching operation of an erbium-doped fiber laser, Laser Phys. Lett. 10 (2013) 075102.
[24] H. Yu, H. Zhang, Z. Wang, J. Wang, Z. Shao, M. Jiang, X. Zhang, CW And Q-switched laser output of LD-end-pumped 1.06μm c-cut nd:$Luvo_4$ laser, Opt. Express 15 (2007) 3206–3211.
[25] X. Zhang, S. Zhao, Q. Wang, Q. Zhang, L. Sun, S. Zhang, Optimization of cr^{4+}-doped saturable-absorber Q-switched lasers, IEEE J. Quantum Electron. 33 (1997) (1997) 2286–2294.
[26] Y. Shimony, Z. Burshtein, Y. Kalisky, Cr^{4+}:YAG as passive Q-switch and brewster plate in a pulsed nd:YAG laser, IEEE J. Quantum Electron. 1995 (31) (1995) 1738–1742.
[27] G. Xiao, J.H. Lim, S. Yang, E.V. Stryland, M. Bass, L. Weichman, Z-scan measurement of the ground and excited state absorption cross sections of cr^{4+} in yttrium aluminum garnet, IEEE J. Quantum Electron. 35 (1999) 1086–1091.
[28] X. Zhang, S. Zhao, Q. Wang, B. Ozygus, H. Weber, Modeling of passively Q-switched lasers, J. Opt. Soc. Amer. B 17 (2000) 1166–1175.
[29] J.E. Ehrlich, D.T. Neilson, A.C. Walker, G.T. Kennedy, A.S. Grant, W. Sibbett, M. Hopkinson, Carrier lifetimes in MBE and MOCVD ingaas quantum wells, Semicond. Sci. Tech. 8 (1993) 307–309.
[30] A.N. Cartwright, D.S. McCallum, T.F. Boggess, A.L. Smirl, T.S. Moise, L.J. Guido, R.C. Barker, B.S. Wherrett, Magnitude, origin, And evolution of piezoelectric optical nonlinearities in strained [111] b ingaas/gaas quantum wells, J. Appl. Phys. 73 (1993) 7767–7774.
[31] A. Szabo, R.A. Stein, Theory of laser giant pulsing by a saturable absorber, J. Appl. Phys. 36 (1965) 1562–1566.
[32] J.J. Degnan, Optimization of passively Q-switched lasers, IEEE J. Quantum Electron. 31 (1995) 1890–1901.
[33] J.J. Degnan, Theory of the optimally coupled Q-switched laser, IEEE J. Quantum Electron. 25 (1989) 214–220.